PHOTOSYNTHETICA
International Journal for Photosynthesis Research

DOI 10.32615/ps.2021.042 PHOTOSYNTHETICA 59 (4): 529-537, 2021

Photosynthetic apparatus performance and anatomical modulations of *Alcantarea imperialis* (Bromeliaceae) exposed to selenium during *in vitro* growth

J.P.R. MARTINS⁺, S.W. MOREIRA, P.C.S. BRAGA, L.T. CONDE, R. CIPRIANO, A.R. FALQUETO, and A.B.P.L. GONTIJO

Department of Agrarian and Biological Sciences, Federal University of Espírito Santo, Litorâneo – 29932-540 São Mateus, ES, Brazil

Abstract

Elements not usually included in culture medium formulations, such as selenium (Se), may have beneficial effects on micropropagated plants. We evaluated the effects of Se on the physiological and anatomical responses of *Alcantarea imperialis* during *in vitro* culture. Plants were cultured in a medium containing a gradient of Se concentrations (0, 4, 8, 16, or 32 µM Se). After 56 d, the growth traits, chlorophyll *a* fluorescence, and root and leaf anatomy were analyzed. The fresh mass declined at the highest Se concentration. Higher Se concentrations induced bigger stomata, while the stomatal density decreased. Plants cultured with Se had improved PSII and PSI electron transport. This led to higher values of the total performance index. Thus, Se-induced plants showed a higher electron transport dynamics and energy conservation from water to PSI and developed anatomical traits that can favor tolerance to water deficit.

Keywords: bromeliad; chlorophyll *a* fluorescence; electron transport; plant anatomy; plant tissue culture.

Introduction

In vitro techniques are often used for large-scale propagation of plants with high economic value or endangered status (Manokari *et al.* 2020, Priyadharshini *et al.* 2020, Kaur *et al.* 2021, Shekhawat *et al.* 2021). These techniques are particularly applied to ornamental species, including members of the Bromeliaceae family (Martins *et al.* 2015,

Highlights

- Plants grown with Se showed an improvement in PSII electron transport
- Se can induce plants with higher PI_{total} values during *in vitro* growth
- Se induced changes in the leaf anatomy benefiting the acclimatization stage

Received 9 June 2021
Accepted 6 September 2021

⁺Corresponding author
phone: +55 27 3121 1696
e-mail: jprmartinss@yahoo.com.br

Abbreviations: Chl – chlorophyll; F_0 – minimal fluorescence yield of the dark-adapted state; F_I – fluorescence intensity at 30 ms; F_J – fluorescence intensity at 2 ms; F_K – fluorescence intensity at 0.3 ms; F_K/F_J – ratio of fluorescence at K and J step of the induction curves; F_L – fluorescence intensity at 0.15 ms; F_m – maximal fluorescence yield of the dark-adapted state; F_P – fluorescence peak; F_t – fluorescence at time t after the beginning of actinic illumination; F_V/F_0 – ratio of the de-excitation rate constants for photochemical and nonphotochemical events; OEC – oxygen-evolving complex; PI_{total} – total performance index, which measures the performance up until the final electron acceptors of PSI; RC/CS_m – total number of PSII active reaction centers; S_m/t_{Fmax} – average fraction of open RC in the period of 0 to t_{Fmax} (time of maximum fluorescence production); V_I – relative variable fluorescence at 30 ms (step I); V_J – relative variable fluorescence at 2 ms (step J); V_K – relative variable fluorescence at 0.3 ms (step K); W_K – the damage to OEC; W_L – indicates disturbance in the thylakoid membranes, reducing the energetic connectivity between the PSII units; δR_0 – efficiency/probability with which an electron from the intersystem electron carriers moves to reduce end electron acceptors at the PSI acceptor side (RE); φD_0 – quantum yield of energy dissipation (at t = 0); φE_0 – quantum yield of electron transport (at t = 0); $\varphi P_0 = F_V/F_m$ – maximum quantum yield of primary photochemistry of PSII reaction center (at t = 0); φR_0 – quantum yield of reduction of end electron acceptors at the PSI acceptor side (RE); ψR_0 – efficiency/probability by which electrons move from PSII to the PSI acceptor side.

Acknowledgments: The authors would like to acknowledge the scholarship awarded by the CAPES (Coordination for the Improvement of Higher Education Personnel) and the FAPES (Espírito Santo State Research Foundation). The authors are also grateful to Luiz Carlos de Almeida Rodrigues for his technical assistance.

Conflict of interest: The authors declare that they have no conflict of interest.

2018; Lando *et al.* 2016, Martínez-Estrada *et al.* 2019, Pakum *et al.* 2021). *Alcantarea imperialis* (Carrière) Harms is among the bromeliad species with ornamental interest. This species is widely employed in landscape projects (Andrade-Santos *et al.* 2021). *A. imperialis* is conventionally propagated by seeds, a method that is not efficient due to low seedling production and the need to conserve seeds. Besides these drawbacks, the plants require several decades to reach adulthood (flowering stage) (Versieux and Wanderley 2015, Tamaki *et al.* 2020). Thus, *in vitro* culture can be an alternative for this species' propagation, as already reported by Mollo *et al.* (2011), Kurita and Tamaki (2014), and Martins *et al.* (2020a). These authors verified the effect of temperature, macronutrients, and plant growth regulators as modulation factors of *in vitro* responses.

The modulation factors can have a negative impact on plant growth while still inside the *in vitro* containers, by inducing physiological disorders. Plants cultured *in vitro* can suffer from nonfunctional stomata, reduced water-use efficiency, and deficiencies in photosynthetic performance (Martins *et al.* 2018, Fortini *et al.* 2021, Shekhawat *et al.* 2021). These morphophysiological characteristics can compromise the final micropropagation step, known as acclimatization. The low capacity of *in vitro* plants to conserve water after transfer to *ex vitro* conditions can lead to desiccation and low survival rates (Asayesh *et al.* 2017). Therefore, the induction of *in vitro* plants with more efficient water use and uncompromised photosynthetic capacity is desirable.

In recent years, the application of elements not usually included in culture medium formulations, such as silicon (Si) and selenium (Se), have been shown to have beneficial effects on plants grown *in vitro* (Martins *et al.* 2019, Souza *et al.* 2019, Seliem *et al.* 2020, Silva *et al.* 2020a). These elements can influence *in vitro* morphogenesis as well as morphophysiology of micropropagated plants (*e.g.*, improve the growth rate and photosynthetic pigment content of *in vitro* plants). The role of Se in the life cycle of plants is still controversial, but several lines of evidence indicate its potential as a biofortification agent when low concentrations are applied (Souza *et al.* 2019, Szarka *et al.* 2020, Sabatino *et al.* 2021). In contrast, Se excess can induce physiological disturbances or even plant death (Sotoodehnia-Korani *et al.* 2020, Szarka *et al.* 2020). Souza *et al.* (2019) and Martins *et al.* (2020b) already have reported the positive effects of Se on the physiological status of a bromeliad species (*Billbergia zebrina*) during *in vitro* culture.

The impacts of *in vitro* conditions can be verified by histological techniques. The characterization of anatomy *via* cross- and paradermical sections has proven to be an important tool to check the effects of culture medium components on *in vitro* plants (Rezende *et al.* 2018, Martins *et al.* 2019, 2020b). Likewise, the photosynthetic performance of *in vitro* plants can be monitored by measurement of chlorophyll (Chl) *a* fluorescence (Martins *et al.* 2018, Rosa *et al.* 2018, Souza *et al.* 2019). This analysis also provides an overview of the stress status of plants through investigation of PSII and PSI performance (Rosa *et al.* 2018, Martins *et al.* 2020b).

Given the above, the study aimed to assess the physiological and anatomical responses of *A. imperialis* in the function of the Se concentrations during *in vitro* culture.

Materials and methods

Culture conditions and Se supplementation: Plants of *Alcantarea imperialis* previously multiplied in an *in vitro* culture medium with no plant growth regulators (Martins *et al.* 2020a) were used as explants. The explants were transferred to 500-ml glass containers holding 50 ml of MS culture medium (Murashige and Skoog 1962) solidified with 5 g L^{-1} agar, supplemented with 30 g L^{-1} sucrose and 0, 4, 8, 16, or 32 µM Se (Na_2SeO_3). Five explants were placed in each glass container. The pH of all media was adjusted to 5.8 before autoclaving at 120°C, for 20 min. After inoculation in a laminar flow cabinet, the plant material was kept in a growth room for 56 d at 25 ± 2°C and 16/8 h light/dark photoperiod, under slim LED lamps (*Blumenau*® 36 W/6500 K) emitting 70 µmol(photon) m^{-2} s^{-1} of PAR.

Growth characteristics: After 56 d, the plants were harvested and washed with distilled water to remove the culture medium adhering to the root surfaces. To determine their growth, 25 plants from each treatment were collected randomly, mixed, and divided into five pooled samples, and weighed on a precision scale. The fresh mass of the shoots (aerial part) and roots (n = 5) was determined separately [g per plant]. The number of roots per plant was also quantified.

Anatomical analysis: To characterize the anatomical changes of the leaves and roots of the plants grown under the *in vitro* conditions in response to the Se treatments, four *A. imperialis* plants from each treatment were used. All the samples were randomly collected after growth for 56 d and were fixed/stored in 50% ethanol. The anatomical characterization was performed by examination of paradermal and cross-sections of leaves. For the roots, we performed cross-sections at 0.5 cm from the root base. All procedures were performed according to Martins *et al.* (2019). All the sections were viewed using a light microscope (*L-2000AFluor*, *Bioval*), and images were captured with a *Leica EC3* camera (*Wetzlar*, Germany). The software *UTHSCSA-Imagetool*® was used to measure the anatomical characteristics shown in the photomicrographs. Two cross-sections per slide were photographed and analyzed per sample. For the characterization of the roots, we measured the thickness of the endodermis and the number of metaxylem vessels. For the leaves, the density of stomata [mm^{-2}] and trichomes [mm^{-2}], stomatal size [mm^2], the thickness of the chlorenchyma [µm], and hydrenchyma [µm] (abaxial and adaxial sides), as well as the number and diameter of vessel elements, were determined (n = 4).

Chl *a* fluorescence measurement: The Chl *a* fluorescence transients (the OJIP curves) were analyzed in 16 randomly selected plants. The measurements were performed after 56 d of Se treatment during *in vitro* culture, between 07:00 and 09:00 h, using a portable *Handy PEA* fluorimeter (*Hansatech*, King's Lynn, Norfolk, UK). The measurements were accomplished on the second completely expanded leaf in the central rosette after being dark-adapted for 30 min using a leaf clip (*Hansatech*). Double normalizations were performed for the O–P and O–I intervals [$V_{OP} = (F_t - F_0)/(F_m - F_0)$ and $V_{OI} = (F_t - F_0)/(F_I - F_0)$, respectively], as well as the kinetic differences between steps O and I [$\Delta V_{OI} = V_{OI(treatment)} - V_{OI(control)}$]. Treatment without Se (0 μM Se) was used as the control. All OJIP curves, as well as the JIP test parameters, were analyzed according to the method proposed by Srivastava and Strasser (1996) and Strasser *et al.* (2004). The $W_L = (F_L - F_0)/(F_K - F_0)$ and $W_K = (F_K - F_0)/(F_J - F_0)$ were calculated according to Wang *et al.* (2016) and Zhang *et al.* (2018).

Statistical analysis: The experimental design was completely randomized, and the resulting data were submitted to analysis of variance (*ANOVA*), while the means (standard error – SE) were compared using *Tukey*'s test at 5% significance. All analyses were performed using the *SISVAR* software.

Results

Growth traits: The Se treatments did not induce any visible physiological disturbances such as chlorosis and necrosis. However, plants grown in the presence of Se were slightly shorter on average, mainly at 32 μM Se. The fresh mass of both aerial parts and roots declined under the highest Se concentration (Fig. 1*A*). The number of roots also decreased under high Se concentrations, although the decreases were only significant when the plants were exposed to 16 and 32 μM Se (Fig. 1*B*).

Analysis of root and leaf anatomy: The treatments did not influence the analyzed traits of root anatomy (Fig. 2*A–E*). The roots had a similar thickness of the endodermis (8.7 ± 0.09 μm) as well as a number of metaxylem vessels (5.7 ± 0.3). However, Se concentrations had a significant impact on the leaf anatomy. The characteristics of stomata showed antagonistic responses. Higher Se concentrations induced bigger stomata, while the number of stomata per area decreased. *A. imperialis* leaves showed closed stomata, irrespective of the treatment. The density of trichomes did not differ between the treatments (Fig. 2*F–J*, Table 1).

The thickness of adaxial hydrenchyma was statistically similar for all treatments. In contrast, Se supplementation increased the abaxial hydrenchyma thickness. The chlorenchyma was thinner under Se exposure. Finally, xylem vessel traits were similar in all Se treatments (Fig. 2*K–T*, Table 1).

Chl *a* fluorescence: The Se concentrations also affected the performance of the photosynthetic apparatus. The values of V_K did not show any differences. On the other hand, the values of V_J and V_I were lower with Se exposure (Fig. 3).

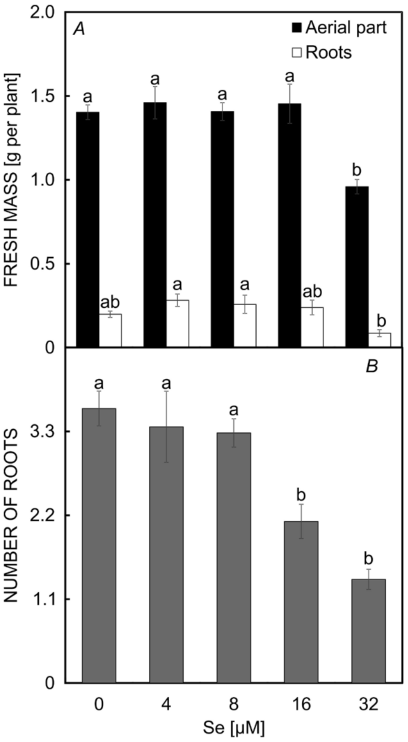

Fig. 1. Fresh mass (*A*) and number of roots (*B*) of *Alcantarea imperialis* plants grown *in vitro* in function of concentrations of Se in the medium. Means ± SE (*n* = 5) followed by *the same letter* do not differ significantly by the *Tukey*'s test ($p<0.05$).

The kinetic differences between the O (20 μs) and I (30 ms) phases were evaluated. All the Se treatments produced negative bands ($V_{OI} \leq 1.0$). The lowest values were observed in the plants cultured with 8 and 16 μM Se (Fig. 4*A*). In addition, the curves of the highest amplitude observed for the relative fluorescence at $V_{OI} \geq 1.0$ were obtained in the interval from 30 to 800 ms for all plants grown with Se (Fig. 4*B*).

Regarding the JIP test parameters, the values of W_L, W_K, F_K/F_J, F_V/F_0, φP_0, φD_0, and RC/CS_m were similar among the treatments. The values of φE_0 were higher in plants under 8 and 16 μM in comparison with the control plants (0 μM Se). Likewise, plants cultured with 4, 8, and 16 μM Se had higher S_m/t_{Fmax} values. The parameters related to PSI activity (φR_0, ψR_0, δR_0) showed increased values in comparison with the plants grown without Se (Fig. 5).

The $\Delta V_{IP} = (F_P - F_I)/(F_P - F_0)$ increased with Se presence (Fig. 6*A*). Likewise, PI_{total} increased gradually with rising Se concentrations, and the highest was in those cultured with 8 and 16 μM Se (Fig. 6*B*).

Discussion

In this study, we report how Se can influence the growth, anatomical and physiological traits of *A. imperialis*.

Plants exposed to concentrations above 16 µM Se showed changes in growth characteristics (fresh mass of aerial part and roots) that could be misinterpreted as a symptom of toxicity induced by excessive Se. In most cases, a reduction of biomass accumulation is the first sign that plants have experienced stressful conditions, and this response normally is correlated with stunted growth and/or physiological disturbances (Kolbert *et al.* 2019, Shafiq *et al.* 2019, Souza *et al.* 2019). The number of roots of *A. imperialis* plants also decreased under high Se concentrations. The root system is highly affected by Se because it usually is the first point of contact with this element in the environment (Kolbert *et al.* 2016). Se can affect root architecture (number and length of lateral roots) since it modulates the expression of genes associated with the biosynthesis of plant hormones (Jia *et al.* 2018, Malheiros *et al.* 2019). Since *A. imperialis* plants did not show clear signs of physiological stress after 56 d of culture, the modulations of the growth traits could be related to another factor. Malheiros *et al.* (2019) observed that Se can interfere with auxin and ethylene balance and also is negatively related to the expression of genes associated with auxin transport. Since auxins are responsible not only for rooting but also for cell enlargement of all plant organs (Tian *et al.* 2018, Toungos 2018, Ma and Li 2019), a decrease in size and mass of *A. imperialis* may be a hormonal response instead of a reflection of stress.

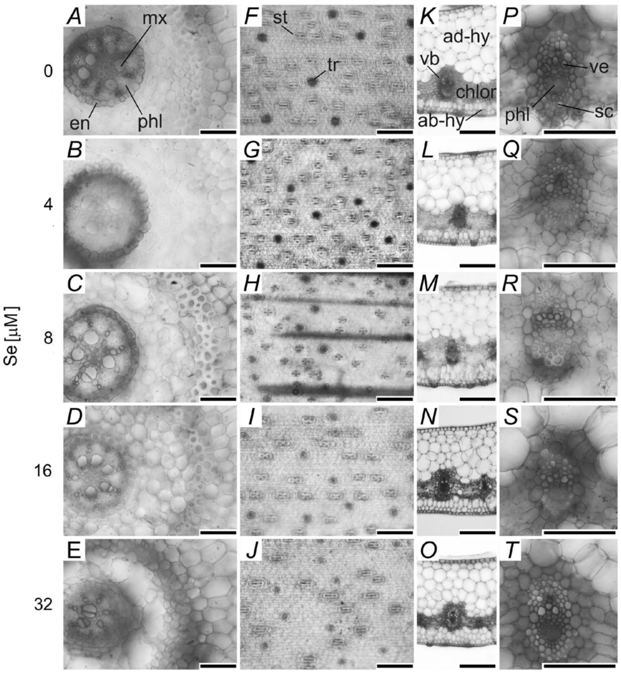

Fig. 2. Paradermal and cross-sections of *Alcantarea imperialis* leaves and roots at 56 d of growth in medium containing 0, 4, 8, 16 or 32 µM Se during *in vitro* culture. ab-hy – abaxial hydrenchyma; ad-hy – adaxial hydrenchyma; chlor – chlorenchyma; en – endodermis; mx – metaxylem vessel; phl – phloem; sc – sclerenchyma; st – stoma; tr – trichome; vb – vascular bundle; ve – vessel element. Bars = 100 µm.

In this work, the leaf and root anatomy of the plants were in accordance with previous reports of *A. imperialis* as well as other species of the Bromeliaceae family (Zorger *et al.* 2019, Martins *et al.* 2020a, Silva *et al.* 2020b, Faria *et al.* 2021). Even though Se modulated the root architecture of *A. imperialis* plants, this metalloid did not interfere with the roots' anatomical traits. Plants under stress promoted by an element (*e.g.*, cadmium, zinc, lead, and sodium) in contact with the roots may show alterations in thickness of the endodermis and/or a number of xylem vessels (Rodrigues *et al.* 2017, Al-Aradi *et al.* 2020, Baroni *et al.* 2020). The endodermis has a protective function because it acts as an apoplastic barrier controlling the radial transport of water and ions, to reduce the entry of contaminants from the surroundings to the vascular cylinder (Rodrigues *et al.* 2017). A smaller number of metaxylem vessels of roots can also act to control element translocation (Martins *et al.* 2016, 2019). Since the plants did not have root anatomical changes associated with Se uptake, the results suggest that stunted growth was not a stress response. The absence of stress was confirmed by the Chl *a* fluorescence analysis. In addition, no changes were found in the xylem traits in the leaves, confirming the plants did not have anatomical mechanisms to regulate Se absorption and translocation.

The Se exposure induced changes in the leaf anatomy that can benefit the acclimatization stage. On the leaf surface, the stomata had characteristics indicating better

Table 1. Anatomical structures of *Alcantarea imperialis* plants grown *in vitro* in function of concentrations of Se [µM] in the medium. For each anatomical trait, means ± SE ($n = 4$) followed by *the same letter* do not differ significantly according to the *Tukey*'s test ($p<0.05$).

Anatomical traits	0 µM Se	4 µM Se	8 µM Se	16 µM Se	32 µM Se
Stomatal size [µm^2]	1,316.5 ± 34.3^b	1,450.6 ± 42.3^{ab}	1,567.0 ± 35.3^a	1,583.8 ± 64.4^a	1,671.9 ± 80.1^a
Stomatal density [mm^{-2}]	66.4 ± 2.9^a	68.2 ± 3.3^a	58.8 ± 5.0^{ab}	35.0 ± 8.7^b	38.7 ± 5.5^b
Density of trichomes [mm^{-2}]	12.1 ± 1.6^a	13.5 ± 1.1^a	12.4 ± 0.7^a	13.7 ± 1.6^a	18.2 ± 2.9^a
Adaxial hydrenchyma [µm]	331.8 ± 34.7^a	313.2 ± 20.0^a	261.3 ± 13.8^a	331.2 ± 17.8^a	301.8 ± 15.4^a
Chlorenchyma [µm]	100.1 ± 2.4^a	85.2 ± 1.8^b	94.8 ± 4.8^{ab}	84.4 ± 3.5^b	81.7 ± 3.0^b
Abaxial hydrenchyma [µm]	73.7 ± 5.2^b	83.9 ± 4.7^{ab}	99.2 ± 2.8^a	97.3 ± 7.7^{ab}	87.2 ± 6.5^{ab}
Diameter of xylem vessels [µm]	8.9 ± 0.1^a	10.5 ± 0.2^a	9.5 ± 0.3^a	9.3 ± 0.5^a	9.7 ± 0.4^a
Number of xylem vessels	3.4 ± 0.8^a	3.7 ± 0.6^a	3.7 ± 0.3^a	3.9 ± 0.4^a	3.4 ± 0.6^a

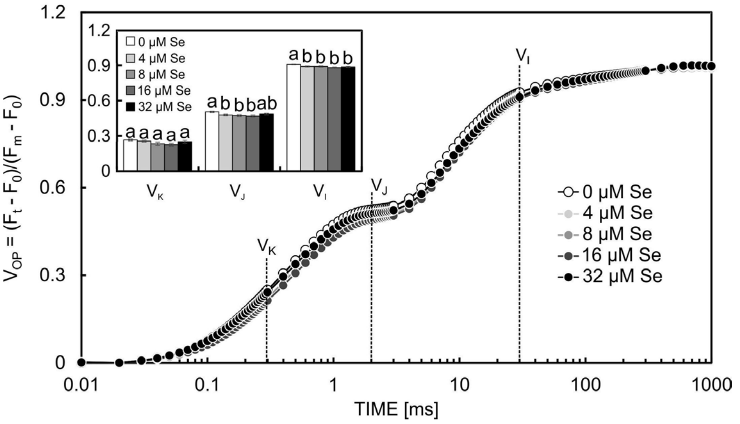

Fig. 3. Relative variable fluorescence between F_0 and F_P (V_{OP}) of *Alcantarea imperialis* plants grown in media with different Se concentrations. For each point of relative variable fluorescence, means ± SE (n = 16) followed by *the same letter* do not differ significantly according to the *Tukey*'s test (p<0.05). V_I – relative variable fluorescence at 30 ms (step I); V_J – relative variable fluorescence at 2 ms (step J); V_K – relative variable fluorescence at 0.3 ms (step K).

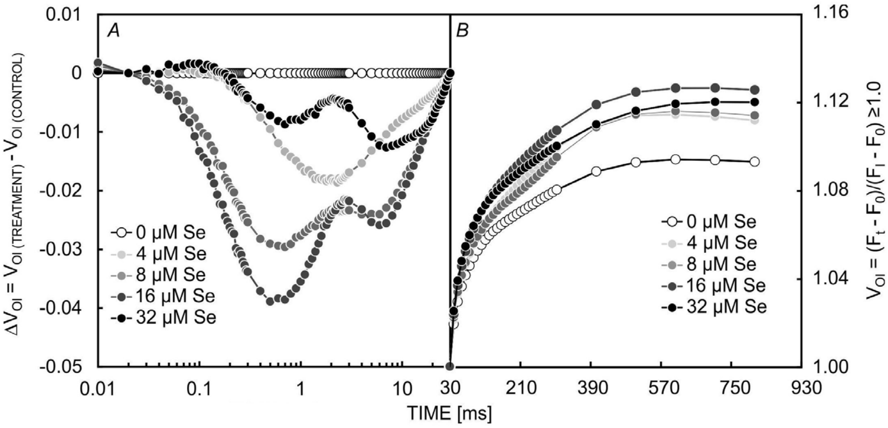

Fig. 4. Chlorophyll *a* fluorescence transient points between the O–I of *Alcantarea imperialis* plants grown in media with different Se concentrations (n = 16). (*A*) Kinetic differences between F_0 and F_I, where $V_{OI} = (F_t - F_0)/(F_I - F_0)$ is $V_{OI} \leq 1$ (range of 0.01 to 30 ms). (*B*) Normalization between F_0 and F_I, where $V_{OI} \geq 1$ is in the range of 30 to 800 ms.

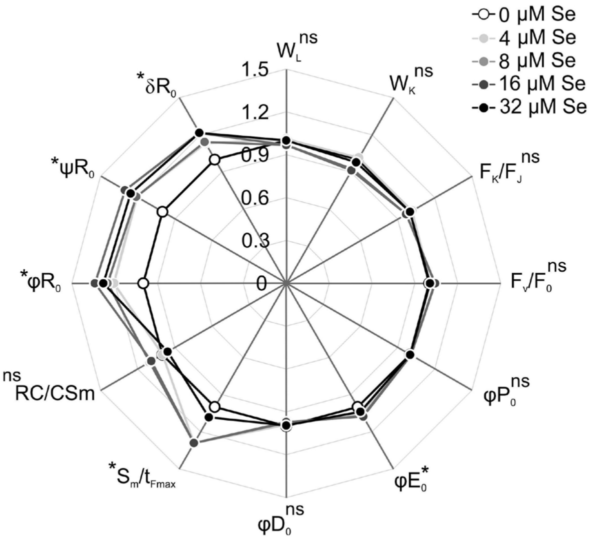

Fig. 5. The JIP test parameters of *Alcantarea imperialis* plants grown in media with different Se concentrations. Means ± SE (n = 16) followed by an asterisk (*) are significantly different according to the *Tukey*'s test (p<0.05). ns – no significant difference. The data were normalized with the control (0 µM Se) equal to 1. F_K/F_J – ratio of fluorescence at K and J step of the induction curves; F_V/F_0 – ratio of the de-excitation rate constants for photochemical and nonphotochemical events; RC/CS_m – total number of PSII active reaction centers; S_m/t_{Fmax} – average fraction of open RC in the period of 0 to t_{Fmax} (time of maximum fluorescence production); W_K – the damage to OEC; W_L – indicates disturbance in the thylakoid membranes, reducing the energetic connectivity between the PSII units; $φP_0$ – maximum quantum yield of primary photochemistry (at t = 0); $φE_0$ – quantum yield of electron transport (at t = 0); $φD_0$ – quantum yield of energy dissipation (at t = 0); $φR_0$ – quantum yield of reduction of end electron acceptors at the PSI acceptor side (RE); $δR_0$ – efficiency/probability with which an electron from the intersystem electron carriers moves to reduce end electron acceptors at the PSI acceptor side (RE); $ψR_0$ – efficiency/probability by which electrons move from PSII to the PSI acceptor side.

water-use efficiency. The stomatal dynamics is the key for water-use efficiency under adverse conditions (Asayesh *et al.* 2017, Kiani-Pouya *et al.* 2019). Regardless of the treatments, all plants showed closed stomata. It can mean the stomata remained functional even under *in vitro* conditions. Nonfunctional stomata (widely open) have often been reported concerning *in vitro* propagated plants, and this anatomical disorder can compromise the acclimatization stage due to faster dehydration of the plants (Manokari *et al.* 2020, Priyadharshini *et al.* 2020, Shekhawat *et al.* 2021). In our work, the stomatal density was negatively correlated with a stomatal size. A reduction in the stomatal density may represent a primary mechanism by which plants can optimize water-use efficiency because

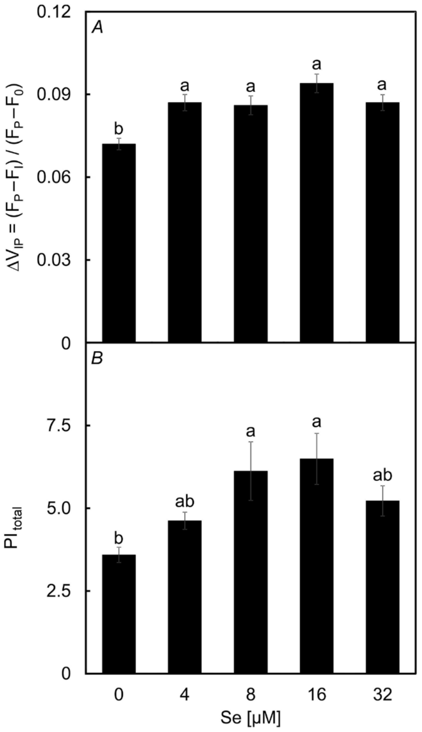

Fig. 6. Relative variable fluorescence between the I–P points (ΔV_{IP}) (*A*) and total performance index (PI_{total}) (*B*) of *Alcantarea imperialis* plants grown *in vitro* in function of concentrations of Se in the medium. Means ± SE ($n = 16$) followed by *the same letter* do not differ significantly according to the *Tukey*'s test ($p<0.05$).

this characteristic can decrease the stomatal conductance (Kiani-Pouya *et al.* 2019). Concerning the stomatal size, it has been reported that bigger stomata have lower water-use efficiency as a function of a slower closing rate (Drake *et al.* 2013, Raven 2014). However, Elliott-Kingston *et al.* (2016) reported that small stomata do not always close faster than large ones. Moreover, smaller stomata do not always favor photosynthesis (Zhang *et al.* 2019). We suggest that an increment in the size of the stomata is a compensation strategy (tradeoff) for reduced stomatal density, which can maintain a proper balance between CO_2 assimilation and water loss. Therefore, the stomatal characteristics presented in *A. imperialis* plants cultured with Se seem to be promising for plants grown under adverse conditions, such as during the initial acclimatization steps.

Still, concerning the water status, bromeliads have a specialized tissue for water storage called hydrenchyma. This tissue can be crucial for *ex vitro* growth after transfer to new conditions by supporting water maintenance (Martins *et al.* 2015, 2018). In this work, the exposure of plants to Se induced leaves with slightly thicker hydrenchyma (abaxial side), which can act to maintain the proper water status. In contrast, plants cultured with Se tended to have thinner chlorenchyma. Although we did not measure the size of the chlorenchyma cells, the number of layers did not vary among the treatments (6–7 cell layers). Thus, the reduction in thickness of this tissue was due to the formation of smaller cells. Smaller Chl parenchyma cells can resist turgor pressure better than large ones. This may offer an advantage under water-deficit conditions by contributing more effectively to turgor maintenance, which can be interpreted as a tolerance mechanism of the leaves to maintain tissue turgor (Boughalleb *et al.* 2015). Therefore, the leaves of *A. imperialis* plants with larger water-storage cells and smaller chlorenchyma cells can be helpful during the stress period that can occur just after transfer to *ex vitro* conditions.

The morphological changes verified after 56 d of culture did not cause physiological disturbances at that time interval. This was demonstrated by the Chl *a* fluorescence transient and parameters of the JIP test. Plants under stress may show lower φP_0 values as well as higher values of φD_0, indicating energy dissipation (Umar *et al.* 2019, Santos *et al.* 2020, Sousaraei *et al.* 2021). According to Bolhar-Nordenkampf *et al.* (1989), plants grown under nonstress conditions usually show values of $\varphi P_0 \geq 0.75$. In this study, the *A. imperialis* plants had φP_0 values greater than 0.78, meaning there was no sign of photoinhibition at 56 d of growth, irrespective of Se treatments. Besides no changes in these parameters, the plants also had similar values of W_L, V_K, F_K/F_J, F_V/F_0, and W_K, together denoting no damage to the functional and structural integrity of the thylakoid membranes and in the oxygen-evolving complex (OEC) (Oukarroum *et al.* 2009, Zhang *et al.* 2018, Faseela *et al.* 2020, Martins *et al.* 2020b).

Plants cultured with Se showed an improvement of PSII electron transport, as indicated by the reduced values of V_J and increased values of φE_0. A decline of the J-step level (V_J) can be attributed to a lower accumulation of reduced plastoquinone A (Q_A) electron acceptor of PSII RC. This is interpreted as a higher rate of electron flow from Q_A to the plastoquinone B (Q_B) electron acceptor of PSII RC and expressed as increased values of φE_0 (Martins *et al.* 2019, Guo *et al.* 2020a). This lower accumulation of Q_A^- was reflected in higher values of S_m/t_{Fmax}. Thus, the higher values of S_m/t_{Fmax}, verified in plants grown with Se, can indicate an accelerated electron transport beyond Q_A^- and a bigger pool of oxidized electron acceptors between PSII and PSI.

The double normalization method allowed us to verify the changes from the I step. The kinetic changes between O and I steps ($V_{OI} \leq 1.0$) can indicate the process of exciton trapping and reduction of plastoquinone pool (Yusuf *et al.* 2010, Khalid *et al.* 2015, Ayyaz *et al.* 2020). The negative amplitudes (displayed as kinetic differences − ΔV_{OI}) verified in plants cultured with Se (Fig. 4*A*) indicated that this element affected the process involving the trapping of the exciton to the reduction of PQ and those plants could maintain the maximum PQ reduction rate (Adamski *et al.* 2011). $V_{OI} \geq 1$ is related to the I–P phase and reveals the changes in the electron flux from the plastoquinol (PQH_2) to the end electron acceptors on the PSI acceptor side (Yusuf *et al.* 2010, Braga *et al.* 2020, Naciri *et al.* 2021). The higher amplitudes observed through the normalization between the O–I steps ($V_{OI} \geq 1.0$) in

Se-treated plants (Fig. 4*B*) are also an indication of the dynamic modulations of the electron transport from the intersystem to the PSI and can be interpreted as an increase in the pool size of the final electron acceptors from the acceptor side of the PSI (Souza *et al.* 2019).

Further regarding step I, decreased values of V_I were observed in *A. imperialis* plants cultured with Se. An increase of V_I may indicate partial inhibition on the acceptor side of PSII due to a relative change in the Q_B-nonreducing PSII RCs (Jiang *et al.* 2008). It can result in a lower efficiency/probability of electron movement from PSII to the PSI acceptor side (Martins *et al.* 2020b). Therefore, the decreased values of V_I, verified in this work, corresponded to a relative improvement of electron transport to PSI, which was reflected in increased values of ψR_0 and φR_0. These results may also reflect the increased electrons flux toward the cyclic flow to improve metabolic energy (ATP) to plants (Fang *et al.* 2020). Lower values of ψR_0 are associated with reduced PSI activity (Rastogi *et al.* 2019, Faseela *et al.* 2020). In our study, *A. imperialis* plants had higher ψR_0 values, which can denote a higher efficiency or probability of trapped electron transfer from PSII to PSI.

The subsequent significant alterations were found in the parameters explaining the state of end electron acceptors on the PSI acceptor side (ΔV_{IP}, φR_0, and δR_0), indicating that Se has potential sites of action in the intersystem and PSI, as suggested by Souza *et al.* (2019). ΔV_{IP} is an indicator of the relative contribution of the I–P phase to the Chl *a* fluorescence emission curve and abundance of PSI with respect to PSII (Ceppi *et al.* 2012, Souza *et al.* 2019). In this study, plants cultured with Se had higher values of ΔV_{IP}, which may have reflected increments in PSI units. These plants also showed higher values of φR_0 and δR_0. These parameters are associated with PSI performance (Lotfi *et al.* 2018, Souza *et al.* 2019, Guo *et al.* 2020b) and have a direct impact on PI_{total} values. Higher values of PI_{total} can indicate an improvement in the potential energy conservation ability of the photons absorbed by PSII for the reduction of the electron acceptors in the intersystem and reduction of the final acceptors in PSI (Yusuf *et al.* 2010). Thus, our results obtained from the J step to P step suggested a greater reduction of the electron transport chain and an enhancement in the transport dynamics and energy conservation of the photosynthetic apparatus, mainly in plants cultured with the concentration range of 8–16 μM Se.

Conclusion: Se can modulate the physiological and anatomical responses of *A. imperialis.* The plants grown without Se exhibited poorer overall performance of photosynthetic apparatus than those cultured with this element. The positive effects of Se exposure during *in vitro* culture were reflected in better transport dynamics and energy conservation from the PSII to PSI, mainly in plants cultured with the concentration range of 8–16 μM Se. In addition, plants cultured with Se exposure showed anatomical traits that can favor the tolerance of water deficit.

References

Adamski J.M., Peters J.A., Danieloski R., Bacarin M.A.: Excess iron-induced changes in the photosynthetic characteristics of sweet potato. – J. Plant Physiol. **168**: 2056-2062, 2011.

Andrade-Santos S.V., Young J.L.M., Ramiro L.K. *et al.*: Effect of nitrate concentration on plant growth and anthocyanin accumulation in the ornamental bromeliad *Alcantarea imperialis*. – J. Plant Nutr. **44**: 181-195, 2021.

Al-Aradi H.J., Al-Najjar M.A., Awad K.M., Abass M.H.: Combination effect between lead and salinity on anatomical structure of date palm *Phoenix dactylifera* L. seedlings. – Agrivita **42**: 487-498, 2020.

Asayesh Z.M., Vahdati K., Aliniaeifard S.: Investigation of physiological components involved in low water conservation capacity of *in vitro* walnut plants. – Sci. Hortic.-Amsterdam **224**: 1-7, 2017.

Ayyaz A., Amir M., Umer S. *et al.*: Melatonin induced changes in photosynthetic efficiency as probed by OJIP associated with improved chromium stress tolerance in canola (*Brassica napus* L.). – Heliyon **6**: e04364, 2020.

Baroni G.D.R., Pereira M.P., Corrêa F.F. *et al.*: Cadmium tolerance during seed germination and seedling growth of *Schinus molle* (Anacardiaceae). – Floresta Ambiente **27**: e20170502, 2020.

Bolhar-Nordenkampf H.R., Long S.P., Baker N.R. *et al.*: Chlorophyll fluorescence as a probe of the photosynthetic competence of leaves in the field: a review of current instrumentation. – Funct. Ecol. **3**: 497-514, 1989.

Boughalleb F., Abdellaoui R., Hadded Z., Neffati M.: Anatomical adaptations of the desert species *Stipa lagascae* against drought stress. – Biologia **70**: 1042-1052, 2015.

Braga P.C.S., Martins J.P.R., Bonomo R. *et al.*: Differential response of photosystem II and I photochemistry in leaves of two *Crambe abyssinica* Hochst lineages submitted to water deficit. – Photosynthetica **58**: 1122-1129, 2020.

Ceppi M.G., Oukarroum A., Çiçek N. *et al.*: The IP amplitude of the fluorescence rise OJIP is sensitive to changes in the photosystem I content of leaves: a study on plants exposed to magnesium and sulfate deficiencies, drought stress and salt stress. – Physiol. Plantarum **144**: 277-288, 2012.

Drake P.L., Froend R.H., Franks P.J.: Smaller, faster stomata: Scaling of stomatal size, rate of response, and stomatal conductance. – J. Exp. Bot. **64**: 495-505, 2013.

Elliott-Kingston C., Haworth M., Yearsley J.M. *et al.*: Does size matter? Atmospheric CO_2 may be a stronger driver of stomatal closing rate than stomatal size in taxa that diversified under low CO_2. – Front. Plant Sci. **7**: 1253, 2016.

Fang Y., Jiang Z., Zhao C. *et al.*: Efficient heat dissipation and cyclic electron flow confer daily air exposure tolerance in the intertidal seagrass *Halophyla beccarii* Asch. – Front. Plant Sci. **11**: 571627, 2020.

Faria C.G., Silva A.S., Melo R.K.P. *et al.*: Leaf anatomy of *Vriesea* (Tillandsioideae–Bromeliaceae). – Brittonia **73**: 27-52, 2021.

Faseela P., Sinisha A.K., Brestič M., Puthur J.T.: Chlorophyll *a* fluorescence parameters as indicators of a particular abiotic stress in rice. – Photosynthetica **58**: 293-300, 2020.

Fortini E.A., Batista D.S., Mamedes-Rodrigues T.C. *et al.*: Gas exchange rates and sucrose concentrations affect plant growth and production of flavonoids in *Vernonia condensata* grown in vitro. – Plant Cell Tiss. Org. Cult. **144**: 593-605, 2021.

Guo Y.Y., Li H.J., Liu J. *et al.*: Melatonin alleviates drought-induced damage of photosynthetic apparatus in maize seedlings. – Russ. J. Plant Physiol. **67**: 312-322, 2020b.

Guo Y., Zhang Y., Lu Y. *et al.*: Effect of AtLFNR1 deficiency on chlorophyll *a* fluorescence rise kinetics OJIP of *Arabidopsis*. – Photosynthetica **58**: 391-398, 2020a.

Jia H., Song Z., Wu F. *et al.*: Low selenium increases the auxin concentration and enhances tolerance to low phosphorous stress in tobacco. – Environ. Exp. Bot. **153**: 127-134, 2018.

Jiang H.X., Chen L.S., Zheng J.G. *et al.*: Aluminum-induced effects on Photosystem II photochemistry in *Citrus* leaves assessed by the chlorophyll *a* fluorescence transient. – Tree Physiol. **28**: 1863-1871, 2008.

Kaur K., Singh P., Kaur K. *et al.*: Development of robust *in vitro* culture protocol for the propagation of genetically and phytochemically stable plants of *Withania somnifera* (L.) Dunal (Ashwagandha). – Ind. Crop. Prod. **166**: 113428, 2021.

Khalid A., Athar H.U.R., Zafar Z.U. *et al.*: Photosynthetic capacity of canola (*Brassica napus* L.) plants as affected by glycinebetaine under salt stress. – J. Appl. Bot. Food Qual. **88**: 78-86, 2015.

Kiani-Pouya A., Rasouli F., Bazihizina N. *et al.*: A large-scale screening of quinoa accessions reveals an important role of epidermal bladder cells and stomatal patterning in salinity tolerance. – Environ. Exp. Bot. **168**: 103885, 2019.

Kolbert Z., Lehotai N., Molnár Á., Feigl G.: "The roots" of selenium toxicity: A new concept. – Plant Signal. Behav. **11**: e1241935, 2016.

Kolbert Z., Molnár Á., Feigl G., Van Hoewyk D.: Plant selenium toxicity: Proteome in the crosshairs. – J. Plant Physiol. **232**: 291-300, 2019.

Kurita F.M.K., Tamaki V.: *In vitro* growth of the bromeliad *Alcantarea imperialis* (Carrière) Harms with different concentrations of nitrogen. – Acta Sci. Biol. Sci. **36**: 279-285, 2014.

Lando A.P., Wolfart M.R., Fermino Jr. P.C.P., Santos M.: Structural effects on *Cattleya xanthina* leaves cultivated *in vitro* and acclimatized *ex vitro*. – Biol. Plantarum **60**: 219-225, 2016.

Lotfi R., Kalaji H.M., Valizadeh G.R. *et al.*: Effects of humic acid on photosynthetic efficiency of rapeseed plants growing under different watering conditions. – Photosynthetica **56**: 962-970, 2018.

Ma L., Li G.: Auxin-dependent cell elongation during the shade avoidance response. – Front. Plant Sci. **10**: 914, 2019.

Malheiros R.S.P., Costa L.C., Ávila R.T. *et al.*: Selenium downregulates auxin and ethylene biosynthesis in rice seedlings to modify primary metabolism and root architecture. – Planta **250**: 333-345, 2019.

Manokari M., Priyadharshini S., Arumugam N., Shekhawat M.S.: Mitigating in vitro induced macro- and micro-morphological anomalies using seismic stress in *Vitex negundo* L. – Plant Cell Tiss. Org. Cult. **143**: 411-420, 2020.

Martínez-Estrada E., Islas-Luna B., Pérez-Sato J.A. *et al.*: Temporary immersion improves *in vitro* multiplication and acclimatization of *Anthurium andreanum* Lind. – Sci. Hortic.-Amsterdam **249**: 185-191, 2019.

Martins J.P.R., Martins A.D., Pires M.F. *et al.*: Anatomical and physiological responses of *Billbergia zebrina* (Bromeliaceae) to copper excess in a controlled microenvironment. – Plant Cell Tiss. Org. Cult. **126**: 43-57, 2016.

Martins J.P.R., Rodrigues L.C.A., Santos E.R. *et al.*: Anatomy and photosystem II activity of *in vitro* grown *Aechmea blanchetiana* as affected by 1-naphthaleneacetic acid. – Biol. Plantarum **62**: 211-221, 2018.

Martins J.P.R., Rodrigues L.C.A., Silva T.S. *et al.*: Sources and concentrations of silicon modulate the physiological and anatomical responses of *Aechmea blanchetiana* (Bromeliaceae) during in vitro culture. – Plant Cell Tiss. Org. Cult. **137**: 397-410, 2019.

Martins J.P.R., Rodrigues L.C.A., Silva T.D.S. *et al.*: Modulation of the anatomical and physiological responses of *in vitro* grown *Alcantarea imperialis* induced by NAA and residual effects of BAP. – Ornam. Hortic. **26**: 283-297, 2020a.

Martins J.P.R., Souza A.F.C., Rodrigues L.C.A. *et al.*: Zinc and selenium as modulating factors of the anatomy and physiology of *Billbergia zebrina* (Bromeliaceae) during *in vitro* culture. – Photosynthetica **58**: 1068-1077, 2020b.

Martins J.P.R., Verdoodt V., Pasqual M., De Proft M.: Impacts of photoautotrophic and photomixotrophic conditions on in vitro propagated *Billbergia zebrina* (Bromeliaceae). – Plant Cell Tiss. Org. Cult. **123**: 121-132, 2015.

Mollo L., Martins M.C.M., Oliveira V.F. *et al.*: Effects of low temperature on growth and non-structural carbohydrates of the imperial bromeliad *Alcantarea imperialis* cultured in vitro. – Plant Cell Tiss. Org. Cult. **107**: 141-149, 2011.

Murashige T., Skoog F.: A revised medium for rapid growth and bio assays with tobacco tissue cultures. – Physiol. Plantarum **15**: 473-497, 1962.

Naciri R., Lahrir M., Benadis C. *et al.*: Interactive effect of potassium and cadmium on growth, root morphology and chlorophyll *a* fluorescence in tomato plant. – Sci. Rep.-UK **11**: 5384, 2021.

Oukarroum A., Schansker G., Strasser R.J.: Drought stress effects on photosystem I content and photosystem II thermotolerance analyzed using Chl *a* fluorescence kinetics in barley varieties differing in their drought tolerance. – Physiol. Plantarum **137**: 188-199, 2009.

Pakum W., Inmano O., Kongbangkerd A.: TDZ and 2,4-D on *in vitro* propagation of panda plant from leaf explants. – Ornam. Hortic. **27**: 41-48, 2021.

Priyadharshini S., Manokari M., Shekhawat M.S.: Attenuation of morpho-anatomical disorders of micropropagated plantlets of *Crinum malabaricum* Lekhak and Yadav using seismo-mechanical stimulation. – Braz. J. Bot. **43**: 969-977, 2020.

Rastogi A., Zivcak M., Tripathi D.K. *et al.*: Phytotoxic effect of silver nanoparticles in *Triticum aestivum*: Improper regulation of photosystem I activity as the reason for oxidative damage in the chloroplast. – Photosynthetica **57**: 209-216, 2019.

Raven J.A.: Speedy small stomata? – J. Exp. Bot. **65**: 1415-1424, 2014.

Rezende R.A.L.S., Rodrigues F.A., Soares J.D.R. *et al.*: Salt stress and exogenous silicon influence physiological and anatomical features of *in vitro*-grown cape gooseberry. – Ciên. Rural **48**: e20170176, 2018.

Rodrigues L.C.A., Martins J.P.R., Almeida Júnior O. *et al.*: Tolerance and potential for bioaccumulation of *Alternanthera tenella* Colla to cadmium under in vitro conditions. – Plant Cell Tiss. Org. Cult. **130**: 507-519, 2017.

Rosa W.S., Martins J.P.R., Rodrigues E.S. *et al.*: Photosynthetic apparatus performance in function of the cytokinins used during the in vitro multiplication of *Aechmea blanchetiana* (Bromeliaceae). – Plant Cell Tiss. Org. Cult. **133**: 339-350, 2018.

Sabatino L., La Bella S., Ntatsi G. *et al.*: Selenium biofortification and grafting modulate plant performance and functional features of cherry tomato grown in a soilless system. – Sci. Hortic.-Amsterdam **285**: 110095, 2021.

Santos E.R., Martins J.P.R., Rodrigues L.C.D.A. *et al.*: Morphophysiological responses of *Billbergia zebrina* Lindl. (Bromeliaceae) in function of types and concentrations of carbohydrates during conventional *in vitro* culture. – Ornam. Hortic. **26**: 18-34, 2020.

Seliem M.K., Abdalla N., El-Ramady H.R.: Response of *Phalaenopsis* orchid to selenium and bio-nano-selenium: *in vitro* rooting and acclimatization. – Environ. Biodivers.

Soil Secur. **4**: 277-290, 2020.

Shafiq S., Adeel M., Raza H. *et al.*: Effects of foliar application of selenium in maize (*Zea mays* L.) under cadmium toxicity. – Biol. Forum **11**: 61-71, 2019.

Shekhawat M.S., Manokari M., Kannan N., Priyadharshini S.: Exogenous implication of seismic stress in attenuation of *in vitro* induced morpho-anatomical aberrations in *Hemidesmus indicus* (L.) R. Br. ex Schult. – S. Afr. J. Bot. **140**: 385-392, 2021.

Silva D.P.C., Oliveira Paiva P.D., Herrera R.C. *et al.*: Effectiveness of silicon sources for in vitro development of gerbera. – Plant Cell Tiss. Org. Cult. **141**: 77-85, 2020a.

Silva E.C., Sibov S.T., Santos F.C.A.D., Gonçalves L.A.: Influence of test tube sealing on the morpho-anatomy and ultrastructure of leaves of *Aechmea bromeliifolia* (Bromeliaceae) grown *in vitro*. – Rodriguésia **71**: e00332018, 2020b.

Sotoodehnia-Korani S., Iranbakhsh A., Ebadi M. *et al.*: Selenium nanoparticles induced variations in growth, morphology, anatomy, biochemistry, gene expression, and epigenetic DNA methylation in *Capsicum annuum*; an in vitro study. – Environ. Pollut. **265**: 114727, 2020.

Sousaraei N., Mashayekhi K., Mousavizadeh S.J. *et al.*: Screening of tomato landraces for drought tolerance based on growth and chlorophyll fluorescence analyses. – Hortic. Environ. Biote. **62**: 521-535, 2021.

Souza A.F.C., Martins J.P.R., Gontijo A.B.P.L., Falqueto A.R.: Selenium improves the transport dynamics and energy conservation of the photosynthetic apparatus of *in vitro* grown *Billbergia zebrina* (Bromeliaceae). – Photosynthetica **57**: 931-941, 2019.

Srivastava A., Strasser R.J.: Stress and stress management of land plants during a regular day. – J. Plant Physiol. **148**: 445, 1996.

Strasser R.J., Tsimilli-Michael M., Srivastava A.: Analysis of the chlorophyll *a* fluorescence transient. – In: Papageorgiou G.C., Govindjee (ed.): Chlorophyll *a* Fluorescence: A Signature of Photosynthesis. Advances in Photosynthesis and Respiration. Pp. 321-362. Springer, Dordrecht 2004.

Szarka V., Jokai Z., El-Ramady H. *et al.*: Biofortification of *Stevia rebaudiana* (Bert.) plant with selenium. – Environ. Biodivers. Soil Secur. **4**: 19-31, 2020.

Tamaki V., Carvalho C.P., Lazarini R.A.D.M. *et al.*: [Storage of seeds harvested from different positions of the floral scape to obtain imperial bromeliad plants – *Alcantarea imperialis*.] – Rodriguésia **71**: e02832018, 2020. [In Portuguese]

Tian H., Lv B., Ding T. *et al.*: Auxin-BR interaction regulates plant growth and development. – Front. Plant Sci. **8**: 2256, 2018.

Toungos M.D.: Plant growth substances in crop production: A review. – Int. J. Innov. Agric. Biol. Res. **6**: 1-8, 2018.

Umar M., Uddin Z., Siddiqui Z.S.: Responses of photosynthetic apparatus in sunflower cultivars to combined drought and salt stress. – Photosynthetica **57**: 627-639, 2019.

Versieux L.M., Wanderley M.G.L.: Bromélias – Gigantes do Brasil. [Giant Bromeliads from Brazil.] Pp. 200. Capim Macio & Offset, Natal 2015. [In Portuguese]

Wang Y.W., Xu C., Lv C.F. *et al.*: Chlorophyll *a* fluorescence analysis of high-yield rice (*Oryza sativa* L.) LYPJ during leaf senescence. – Photosynthetica **54**: 422-429, 2016.

Yusuf M.A., Kumar D., Rajwanshi R. *et al.*: Overexpression of γ-tocopherol methyl transferase gene in transgenic *Brassica juncea* plants alleviates abiotic stress: Physiological and chlorophyll *a* fluorescence measurements. – BBA-Bioenergetics **1797**: 1428-1438, 2010.

Zhang H.H., Xu N., Wu X. *et al.*: Effects of four types of sodium salt stress on plant growth and photosynthetic apparatus in sorghum leaves. – J. Plant Interact. **13**: 506-513, 2018.

Zhang Q., Peng S., Li Y.: Increase rate of light-induced stomatal conductance is related to stomatal size in the genus *Oryza*. – J. Exp. Bot. **70**: 5259-5269, 2019.

Zorger B.B., Arrivabene H.P. Milanez C.R.D.: Adaptive morphoanatomy and ecophysiology of *Billbergia euphemiae*, a hemiepiphyte Bromeliaceae. – Rodriguésia **70**: e00592018, 2019.